Simulation analysis and design of electron deflector for eXTP focusing telescope*

ZHENG Renzhou[1], QIANG Pengfei[1], YANG Yanji[2], YAN Yongqing[1,*], LI Yue[1], SHENG Lizhi[1,*], CHEN Yong[2]

1.State Key Laboratory of Transient Optics and Photonics, Xi'an Institute of Optics and Precision Mechanics, Chinese Academy of Sciences, Xi'an 710119, China

2.Key Laboratory of Particle Astrophysics, Institute of High Energy Physics, Chinese Academy of Sciences, Beijing 100049, China

Abstract

X-ray focusing telescope is the core equipment for space X-ray observation. In order to ensure the accuracy of the observation results, it is necessary to deflect the low-energy electrons entering the focusing telescope to effectively reduce the background noise. In this work, the electron deflector for enhanced X-ray timing and polarimetry mission (eXTP) focusing telescope is developed to meet the deflection requirements of low-energy electrons in the focusing telescope optical system, with the lightweight, ability to deflect electrons , and electromagnetic compatibility considered. The finite element analysis software COMSOL Multiphysics is used to establish the full physical simulation model of the electron deflector and focusing telescope mirrors. The magnetic flux density distribution, electron deflection trajectories and the effect of magnetic field on focusing telescope mirrors are analyzed, and the electromagnetic parameters of the electron deflector are designed. The simulation results show that the closer to the magnet and the center of electron deflector, the greater the magnetic flux density, and the maximum magnetic flux density in the middle of the two spokes can reach 0.027 T. When the radius is larger than 280 mm, the longitudinal distance is larger than 60 mm, the magnetic flux density is less than 5×10^{-5} T (0.5 Gs), i.e. the geomagnetic intensity, which meets the design requirements of electromagnetic compatibility performance. When the incidence angle is ≤10°, the electron deflection efficiency decreases with the increase of electron energy and incidence angle, and the deflection efficiency of electrons below 50 keV

*This paper is a translated version of the original Chinese paper published in Acta Physica Sinica. Please cite the paper as: ZHENG Renzhou, QIANG Pengfei, YANG Yanji, YAN Yongqing, LI Yue, SHENG Lizhi, CHEN Yong, **Simulation analysis and design of electron deflector for eXTP focusing telescope.** *Acta Phys. Sin.* 2025, 74(5): 059502.doi: 10.7498/aps.74.20241649

energy can reach 100%, which meets the design requirements of electron deflection. In addition, as the focusing telescope mirrors are away from the electron deflector, the area of mirrors affected by the magnetic field becomes smaller and smaller. When the distance between the mirror bottom and electron deflector is 130 mm, the magnetic flux density at the mirror bottom only reaches 10^{-4} T. Similarly, as the focusing telescope mirrors are away from the electron deflector, the stress at the mirror bottom decreases from 10^{3} N/m^2 at 10 mm to 10^{-2} N/m^2 at 60 mm, and the deformation at mirror bottom decreases from ~nm at 10 mm to 10^{-4} nm at 60 mm. When the distance between the mirror bottom and electron deflector is 130 mm, the stress is only 10^{-3} N/m^2, and the deformation is only 10^{-5} nm, indicating that the magnetic field does not affect the optical properties of the focusing telescope. The above simulation analyses show that the design parameters of NdFeB magnet structure of the electron deflector fully meet the requirements of the eXTP focusing telescope optical system for the deflection of low-energy electrons. And the deflection efficiency of electrons with 25 keV energy, incidence angle within ±5°, and deflection distance of 5250 mm is 100%. These results provide an important reference for developing electron deflector of eXTP focusing telescope.

Keywords: focusing telescope; electron deflector; magnetic field; deflection efficiency; deformation
PACS: 95.55.Ka; 07.55.Db
doi: 10.7498/aps.74.20241649
cstr: 32037.14.aps.74.20241649

1. Introduction

The two main directions of modern physics research have become the origin of life and the origin of the universe. As an important part of full-band observation, space X-ray observation is an important means of astrophysics and space astronomy research, accounting for about half of space astronomical satellites. NASA and ESA's strategic plan for astronomy in the next 20 years includes the search for stars, galaxies and black holes, the search for habitable terrestrial planets outside the solar system, and the revelation of the basic physical laws of the universe. China has also made a layout in relevant aspects, planning to carry out space science research such as one black (black hole), two dark (dark matter, dark energy), three origins (universe, celestial body, origin of extragalactic life) from 2016 to 2030[1–4].

X-ray focusing telescope is the core equipment for space X-ray observation. However, in the space orbit, electrons will generate noise background[5] in the detector. Therefore, it is usually necessary to install an electron deflector in front of the detector to deflect the space electrons, so that the electrons incident along the focusing mirror are deflected and cannot be incident on the focal plane detector, thus effectively reducing the background noise generated by charged particles such as electrons. The schematic diagram of the structure is shown in Fig.1[6]. The electron deflector generally comprises a hub and a plurality of spokes, wherein a plurality of permanent magnets are arranged on each spoke, and a static magnetic field is formed between adjacent spokes, so that electrons entering the region are deflected and cannot enter the focal plane detector. The Einstein Probe (EP) satellite launched by China on January 9, 2024 and the payloads of foreign satellites such as Swift, eROSITA, XMM-Newton and ATHENA are all designed with electronic deflectors[7–15]. The Einstein Probe satellite carries a (wide-field X-ray telescope WXT) and two (follow-up X-ray telescopes FXT). The electron deflector of WXT is designed with a circular magnetic field to reduce the magnetic leakage and magnetic moment. Sixteen identical rectangular NdFeB permanent magnets are installed in a square frame in a certain order. Every four permanent magnets have the same magnetization direction, and two adjacent permanent magnets have a phase difference of 90 °. In the design process, the structure of the electron deflector is optimized by simulating the electron motion path, and the deflection path length of the electron passing through the magnetic field region is reduced[14]. The electronic deflector of FXT adopts the design of ring spoke magnet. The outer frame is a ring spoke structure. Five specifications of NdFeB permanent magnet blocks are arranged on each of the 16 spokes. The magnetization direction is perpendicular to the radius. The phase difference of the magnetization direction of each specification of permanent magnet block along the ring direction is 22.5 °, and the total magnetic moment is zero. The electronic deflection efficiency of 25 keV, incident angle ± 5 ° and deflection distance 1120 mm is 100%. The magnetic deflector used on the ATHENA (wide field imager WFI) has a magnetic field strength of 0.38 T and a height of 5 cm, which can effectively deflect 76 keV protons[16]. The magnetic deflector of SIMBOL-X telescope also adopts the design of ring spoke magnet. Three NdFeB permanent magnets are arranged on each of the 24 spokes, and the maximum energy of proton deflection can reach 25 keV[13]. In these studies, the motion path and deflection efficiency of charged particles in the magnetic field were simulated and analyzed, and the structure design of the magnetic deflector was further completed. However, there is little discussion about the influence of magnetic field on the optical system, which makes it difficult to provide effective guidance for the evaluation of the performance change of the optical system and the selection of the installation position of the magnetic deflector, so it is necessary to carry out more in-depth research on related aspects.

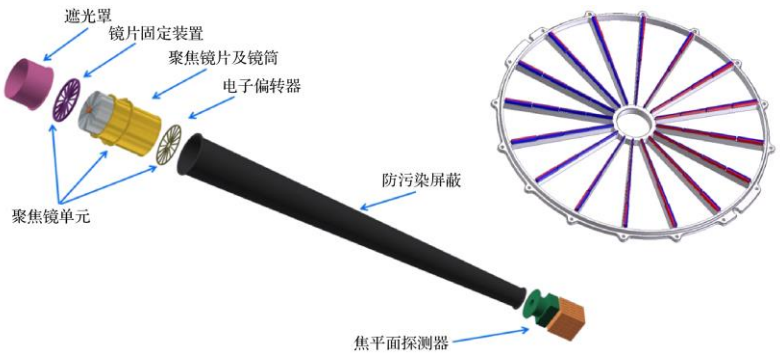

Figure 1. Schematic diagram of the structure of focusing telescope and electron deflector[6].

The enhanced X-ray timing and polarimetry mission (eXTP) is China's next-generation flagship X-ray astronomy satellite after the Hard X-ray Modulation Telescope (HXMT) -Wise Eye satellite. Its core scientific objectives can be summarized as "one odd (black hole), two stars (neutron star and quark star), and three extremes (extreme gravity, magnetic field, and density)". EXTP plans to deploy two payloads: the spectroscopic focusing array (SFA) and the polarimetry focusing array (PFA), which will also use an electronic deflector design[6,17,18].

In this paper, the finite element analysis software COMSOL Multiphysics is used to establish the physical simulation model of the electronic deflector and the focusing mirror, and to complete the electromagnetic parameters design of the electronic deflector, aiming at the development of the eXTP focusing mirror electronic deflector, taking into account the lightweight, electronic deflection capability and electromagnetic compatibility performance. Firstly, the distribution of magnetic induction intensity in the space around the magnet is analyzed, the effective action area of the magnetic field on the electron deflection is defined, and the plane and longitudinal magnetic flux leakage of the electron deflector is checked; Furthermore, by simulating the deflection trajectory of electrons entering the magnetic field region, the change law of electron deflection efficiency is quantified, and the index parameters of the electron deflector are verified; Finally, according to the magnetization process of the focusing lens in the magnetic field, the magnetic induction intensity distribution, stress distribution, deformation size of the focusing lens and the change law of the above key parameters when the distance between the focusing lens and the electronic deflector is changed are analyzed, which provides a reference for the evaluation of the optical performance of the focusing mirror and the selection of the installation position of the electronic deflector.

2. Simulation Design of Electronic Deflector

2.1 Technical specifications of electronic deflector

Xi'an Institute of Optics and Fine Mechanics, Chinese Academy of Sciences, is responsible for the development of the electronic deflector of the X-ray focusing mirror in the "Enhanced X-ray Time-Varying and Polarization Probing (eXTP) Space Observatory" project. In order to ensure the accuracy of the eXTP focusing mirror observation results, it is necessary to effectively deflect the low-energy electrons entering the focusing mirror to achieve the purpose of reducing the background noise. According to the deflection requirements of the eXTP focusing mirror optical system for low-energy electrons, the following conditions shall be met for the design of the electron deflector:

1) Deflectable electron energy shall not be less than 25 keV according to the satellite orbit altitude and the[18] of space electron energy and flux distribution;

2) accord to that geometric structure of the multilayer nested len of the focusing lens, the included angle between the electron emitted through the lens gap and the optical axis of the focusing lens is not more than 5 degrees, and the incident angle of the deflected electrons is within ± 5 degrees;

3) The focal length of the focusing mirror is 5250 mm, the focal plane detector is 5250 mm away from the focusing mirror, and the electrons should be completely deflected within a distance of 5250 mm;

4) The electron deflection efficiency shall be 100%.

2.2 Electron deflector material

The flange of the electronic deflector is made of aluminum alloy, and the model is AA7075, which has high structural strength and meets the mechanical conditions of the satellite. At the same time, AA7075 is made of non-magnetic material, and the relative permeability is 1, which has no effect on the magnetic induction distribution of the magnet. The magnet material is NdFeB material with strong magnetism. The alpha magnetic spectrometer (AMS) in the United States uses NdFeB permanent magnet. After 20 years, no obvious magnetic field attenuation[19,20] has been found, which indicates that the operation life of NdFeB material in the outer space environment can meet the overall requirements of the system. The screw is made of titanium alloy, and the model is TC4. The adhesive is EC2216, and its shear strength can reach 26 MPa, which can ensure the stability of the whole structure. Other material parameters are shown in the Tab.1.

Table 1. Material parameters of the electron deflector.

Name	Material/Type	Quantity	Density/ (kg · m^{-3})	Young's modulus/ (N · mm^{-2})	Poisson's ratio	Mass/kg
Electronic deflector flange	AA7075	1	2800	70000	0.33	0.339
Magnet	NdFeB	120	7400	140000	—	0.224
Screw	TC4	—	7900	210000	0.3	0.003
Adhesive	EC2216	—	—	—	—	—

2.3 Design Scheme of Electromagnetic Parameters of Electronic Deflector

2.3.1 Physical simulation model of electronic deflector

The finite element analysis software COMSOL Multiphysics is used to establish the full physical simulation model of the electronic deflector and the focusing lens, as shown in Fig.2. Combined with the annular structure of the focusing lens, the electronic deflector adopts an axisymmetric annular magnetic field design, five magnets are bonded on each spoke, the number of spokes is 24, which is the same as the number of spokes of the focusing lens, and there is no shielding of X-rays, which can ensure that the effective area of the focusing mirror is not affected. Wolter-1 focusing lens is composed of paraboloid and hyperboloid, both of which are confocal. The lens material is nickel metal. The aperture of the outermost lens is Φ492 mm, and the length of the lens is 600 mm (300 mm paraboloid lens + 300 mm hyperboloid lens). The structural parameters of the NdFeB magnet for the electronic deflector are preliminarily designed after comprehensively considering the aperture of the focusing lens (the magnet covering aperture is Φ175 mm — Φ459 mm), the spoke width (the maximum width of the magnet is 4 mm), the structural strength of the magnet (the minimum width of the magnet is 1.8 mm), and the difficulty of magnet bonding (the distance between the magnets is 2 mm) and after several rounds of electromagnetic parameter simulation iterations, as shown in the Tab.2. Through the multi-physical field coupling simulation of magnetic field and particle tracking, the magnetic induction intensity distribution in the space around the magnet, the deflection trajectory of electrons entering the magnetic field area and the influence of the magnetic field on the focusing lens are analyzed.

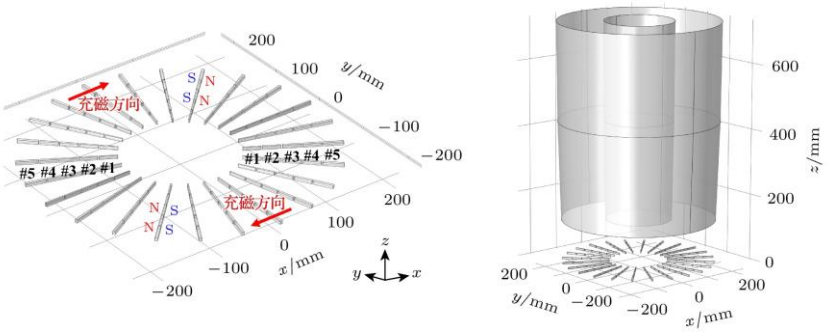

Figure 2. Full physical simulation model of the electron deflector and focusing telescope mirrors.

Table 2. Structure design parameters of the electron deflector NdFeB magnet.

Serial number	Length/mm	Width/mm	Height/mm	Remanence/T
#1	26	1.8	5	1.4
#2	26	2.5	5	1.4
#3	26	3	5	1.4
#4	26	3.5	5	1.4
#5	30	4	5	1.4

2.3.2 Distribution of magnetic induction

The Fig. 3(a) shows the magnetic induction distribution in the space around the electron deflector, and the Fig. 3(b) shows the direction of the magnetic field, which is clockwise when viewed along the electron incident direction. The magnetic induction intensity distribution on the plane where the center of the magnet is located is shown inFig. 4(a), and the magnetic induction intensity x component and y component distributions are shown in Fig. 4(b) and(c), respectively. It can be seen that the closer to the magnet and the center, the greater the magnetic induction intensity is; The x component of magnetic induction on both sides of the x axis is in opposite direction, and the y component of magnetic induction on both sides of the y axis is in opposite direction, which conforms to the clockwise distribution. The distribution of magnetic induction along the radius between two spokes is given by Fig. 5. The magnetic induction decreases along the radius, and the maximum magnetic induction in the middle of two spokes is 0.027T. It is worth noting that the magnetic induction at the symmetry axis of the sector formed by adjacent spokes is

weaker than that in other radial directions, so special attention should be paid to the electron deflection in this region.

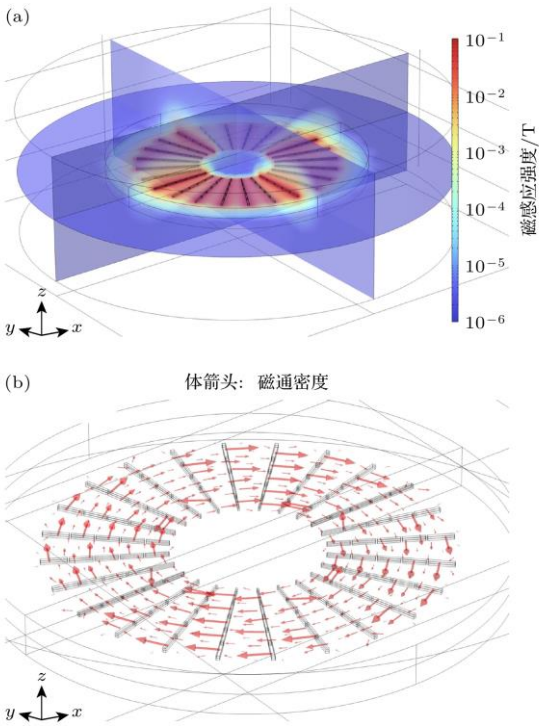

Figure 3. (a) Distribution of magnetic flux density, the color legend on the right represents the magnetic flux density; (b) magnetic field direction around the electron deflector.

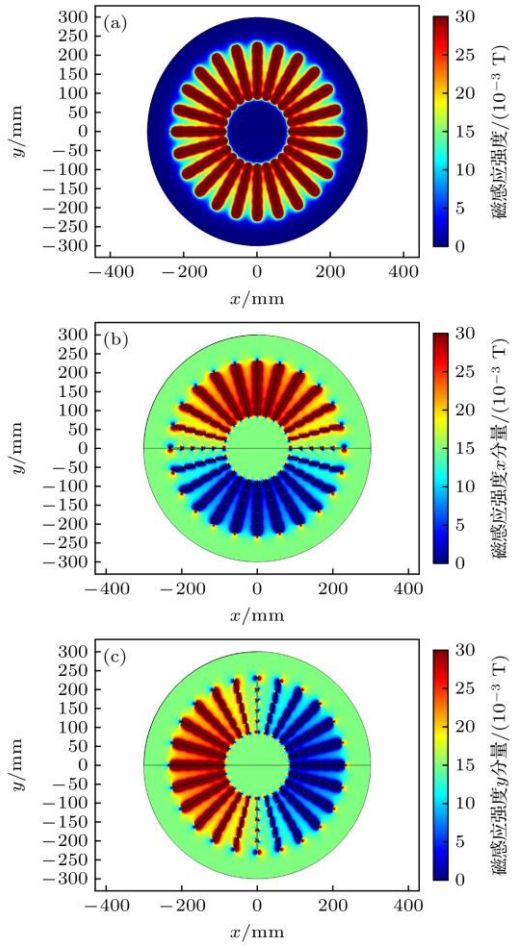

Figure 4. Distribution of (a) magnetic flux density; (b) *x* component of magnetic flux density; (c) *y* component of magnetic flux density in the magnet center plane.

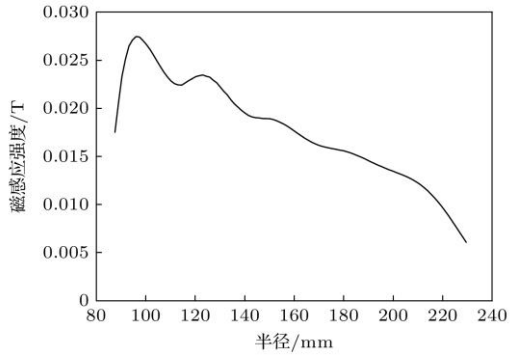

Figure 5. Distribution of magnetic flux density along the radius between two spokes.

According to the requirements of the whole satellite system, the magnetic induction intensity outside a certain area of the focusing mirror electronic deflector should be less than 0.5 Gs (1 Gs = 10^{-4} T), that is, the geomagnetic intensity, so that it has no effect on the magnetic sensitive components of other components in the whole satellite system. Therefore, it is necessary to check the plane and longitudinal magnetic flux leakage of the electronic deflector. The Fig. 6 shows the planar distribution of the magnetic induction within a radius of 500 mm, and the magnetic induction is less than 5×10^{-5} T (0.5 Gs) for a radius greater than 280 mm, indicating that the effect on the surrounding equipment is

negligible. The Fig. 7 shows the longitudinal distribution of magnetic induction intensity, the distance is greater than 60 mm, and the magnetic induction intensity is less than 5 × 10^{-5} T, which meets the design requirements of electromagnetic compatibility.

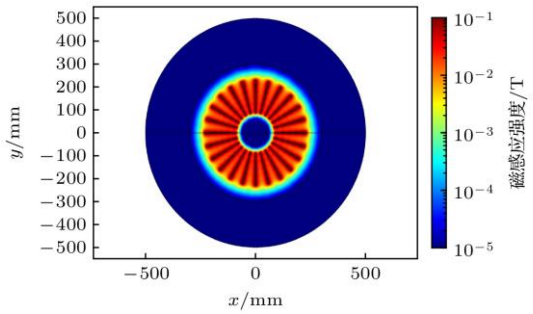

Figure 6. Plane distribution of magnetic flux density within a radius of 500 mm.

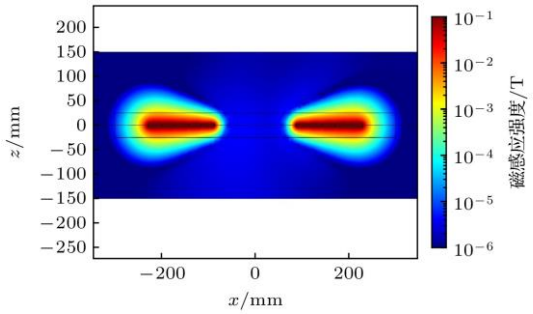

Figure 7. Longitudinal distribution of magnetic flux density.

2.3.3 Electron deflection trajectory

The Fig. 8 shows the relationship between the electron deflection efficiency and the electron energy and the incident angle. The electron deflection efficiency is defined as the ratio of the number of electrons that do not reach the electron collection surface of $\Phi 500$ mm at 5250 mm below the electron deflector to the total number of incident electrons after being deflected by the magnetic field. The incident angle is defined as the angle between the incident direction of electrons and the optical axis of the focusing mirror. It can be seen that the electron deflection efficiency decreases with the increase of electron energy and incident angle when the incident angle is less than 10 °, and the electron deflection efficiency can reach 100% below 50 keV, which meets the design requirements. It can also be seen that for the limit case of 20 ° incident angle, the electron deflection efficiency first decreases and then increases with the increase of electron energy, which is related to the fact that the incident electron (100 keV) on one side (left side) is not deflected from the same side but directly emitted from the other side (right side), as shown in the Fig. 9.

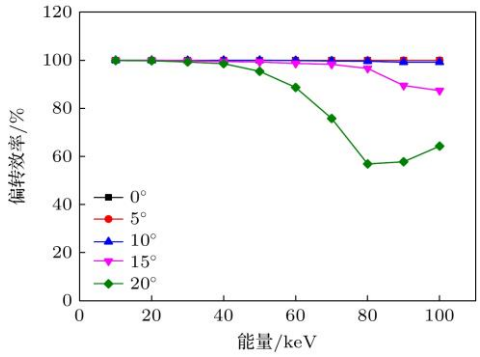

Figure 8. Variations of electron deflection efficiency dependent on the electron energy and incidence angle.

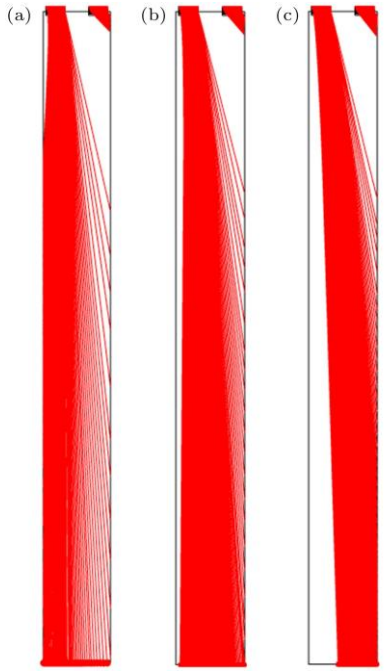

Figure 9. For the 20° incident angle limit case: (a) 60 keV; (b) 80 keV; (c) 100 keV electron deflection trajectories.

The Fig.10 shows the relationship between the electron deflection efficiency and the height of the NdFeB magnet at an incident angle of 5 °. It can be seen that when the height of the NdFeB magnet is reduced to 2 mm, the electron deflection efficiency decreases significantly. In order to ensure that the deflection efficiency of electrons with different energies is 100%, the height of the NdFeB magnet should be 5 mm. Considering the aperture of the focusing lens and the width of the spoke (to ensure the effective area of the focusing lens), the optimization space of the length and width of NdFeB magnet is small, and the structural parameters of NdFeB magnet in the Tab.2 are the ideal optimization results.

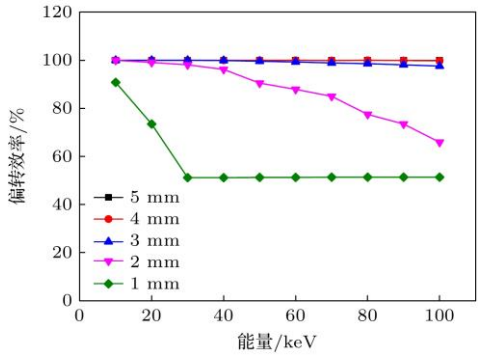

Figure 10. Variations of electron deflection efficiency dependent on the NdFeB magnet height at incident angle of 5°.

2.3.4 Effect of magnetic field on focusing lens

In order to evaluate the influence of the electronic deflector on the optical performance of the focusing lens, it is necessary to simulate and analyze the magnetic induction intensity distribution, stress distribution and deformation size of the focusing lens under the action of the magnetic field. As shown in Fig.11, the magnetic induction intensity distribution of the focusing lens when the bottom of the focusing lens is 130 mm away from the electronic deflector. The lens is made of nickel metal, and the magnetic induction intensity at the bottom of the focusing mirror is only 10^{-4} T. As shown in the Fig.12, the magnetic induction intensity distribution of the space around the electronic deflector and the focusing lens, due to magnetization, the magnetic induction intensity of the lens is greater than that of the surrounding space; Due to the magnetic shielding effect, the magnetic induction between the lenses is less than that in the surrounding space.

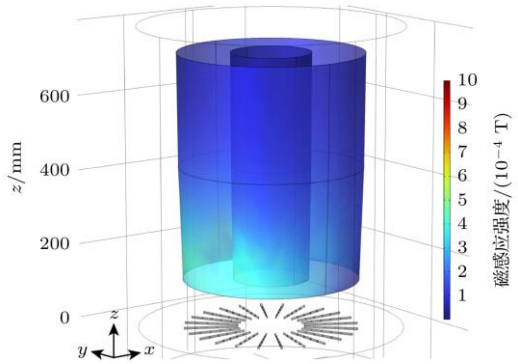

Figure 11. Distribution of magnetic flux density of the focusing telescope mirrors.

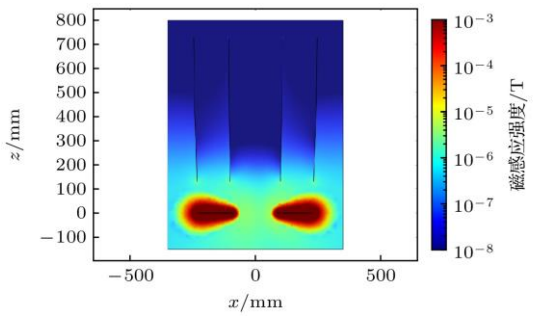

Figure 12. Distribution of magnetic flux density around the electron deflector and focusing telescope mirrors.

The Fig.13 shows the stress distribution of the focusing lens, and the stress magnitude is only 10^{-3} N/m^2. As shown in Fig.14(a), it is the deformation of the focusing lens, and as shown in Fig.14(b) —(d), it is the x component, y component and z component of the lens deformation, respectively. It can be seen that the lens deformation is mainly distributed in the x direction and y direction, that is, the lens shrinks inward; The deformation is only 10^{-5} nm, and in the optical design of the focusing mirror, the surface error of the mirror is required to be less than 1 μm and the roughness is required to be less than 0. 4 nm, so the magnetic field of the electronic deflector will not affect the optical performance of the focusing mirror.

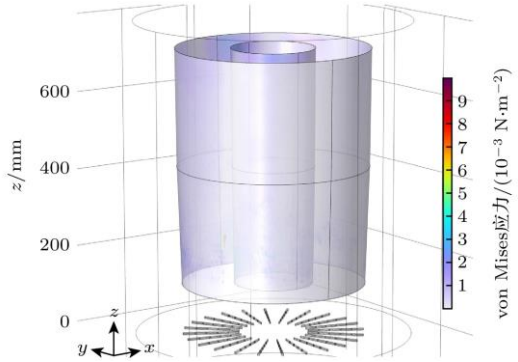

Figure 13. Stress distribution of the focusing telescope mirrors.

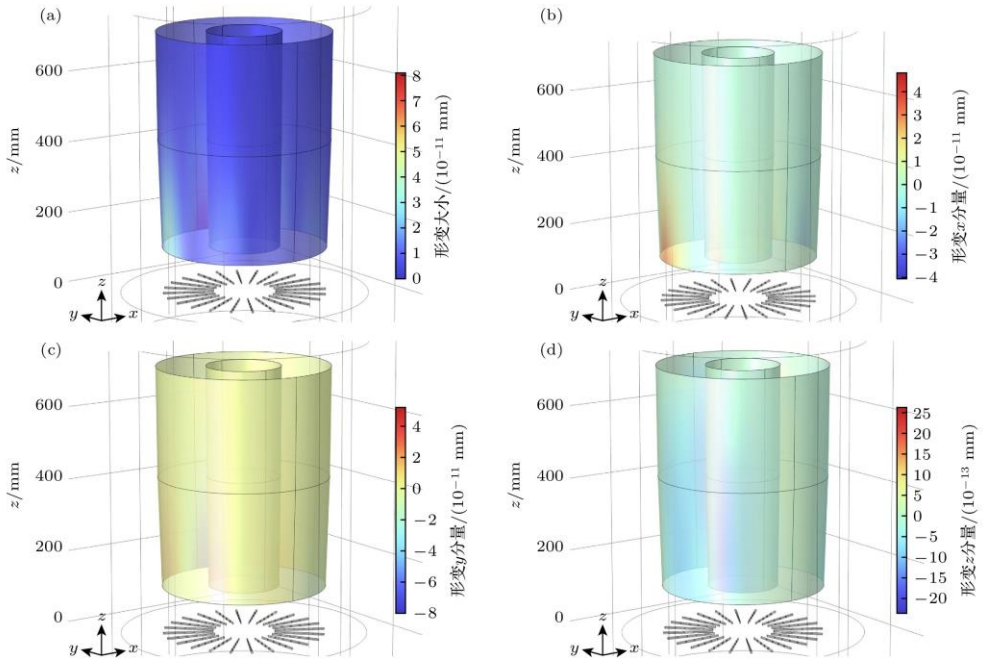

Figure 14. (a) Deformation, (b) *x* component of deformation, (c) *y* component of deformation, and (d) *z* component of deformation of the focusing telescope mirrors.

Fig.15 shows the magnetic induction distribution of the focusing lens at different distances from the bottom of the focusing lens to the electronic deflector. As the focusing lens is far away from the electronic deflector, the area of the lens affected by the magnetic field becomes smaller and smaller.

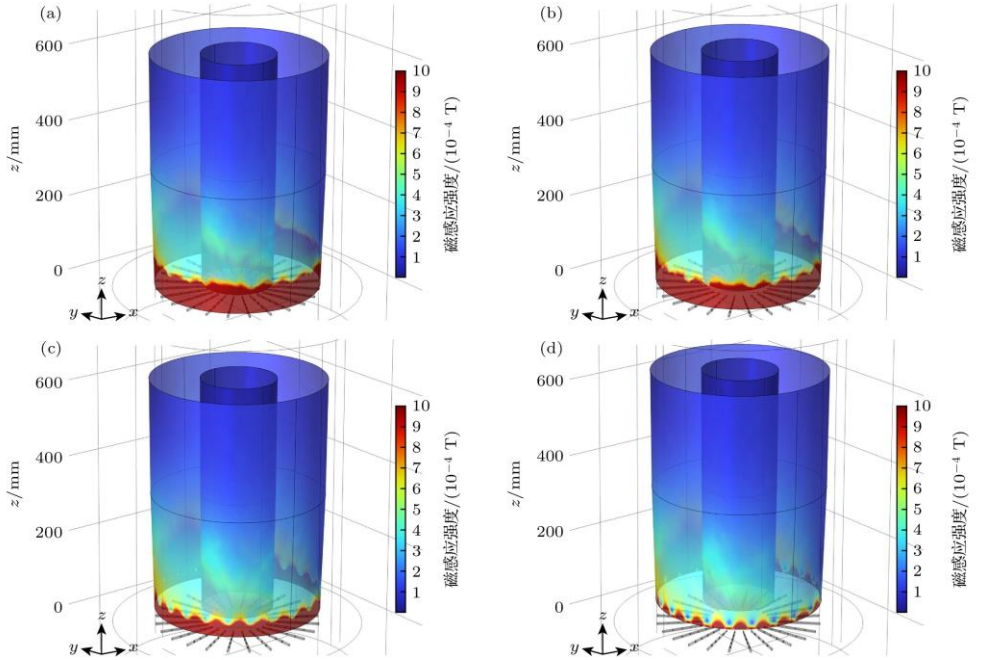

Figure 15. Distribution of magnetic flux density of the focusing telescope mirrors when the distance between the mirror bottom and electron deflector is (a) 10 mm, (b) 20 mm, (c) 40 mm, and (d) 60 mm.

The Fig.16 shows the magnetic induction intensity distribution in the space around the electronic deflector and the focusing lens at different distances from the bottom of the focusing lens. It can be seen that the focusing lens will affect the magnetic induction intensity distribution in the space around the electronic deflector. With the reduction of the distance between the two, the spatial magnetic induction intensity will become more and more asymmetric.

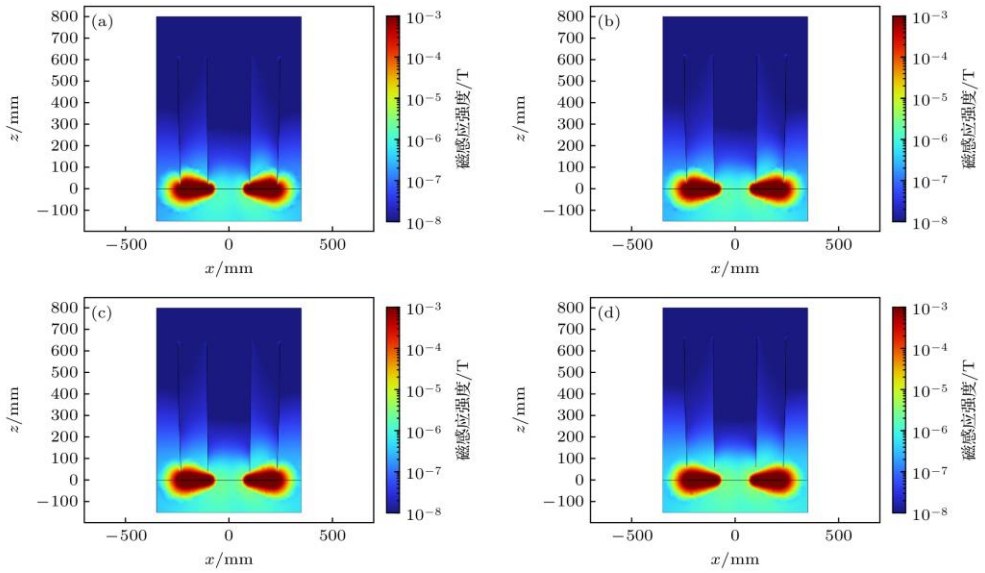

Figure 16. Distribution of magnetic flux density around the electron deflector and focusing telescope mirrors when the distance between the mirror bottom and electron deflector is (a) 10 mm, (b) 20 mm, (c) 40 mm, and (d) 60 mm.

The Fig.17 shows the stress distribution of the focusing lens at different distances from the electronic deflector. As the focusing lens is far away from the electronic deflector, the stress at the bottom of the lens decreases from 10^3 N/m^2 at 10 mm to 10^{-2} N/m^2 at 60 mm.

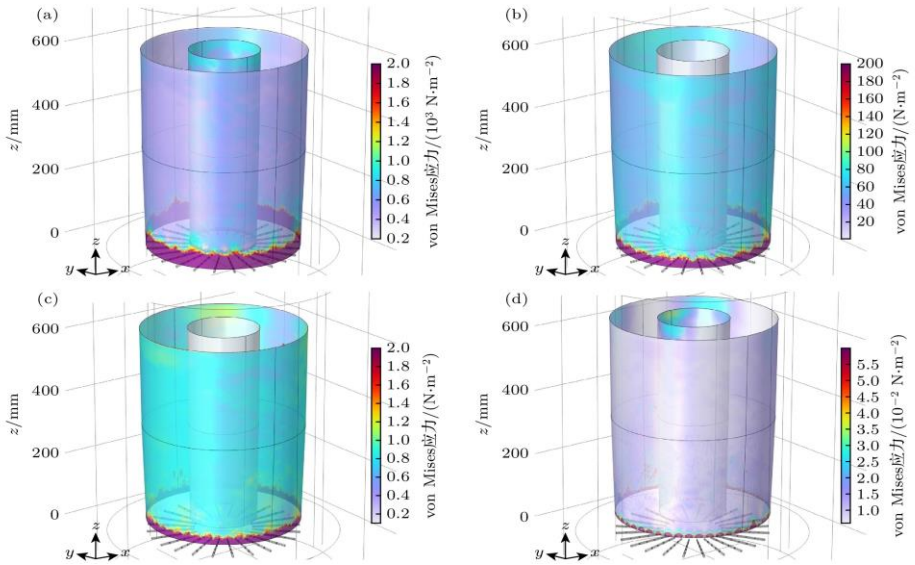

Figure 17. Stress distribution of the focusing telescope mirrors when the distance between the mirror bottom and electron deflector is (a) 10 mm, (b) 20 mm, (c) 40 mm, and (d) 60 mm.

The Fig.18 shows the deformation of the focusing lens at different distances from the electronic deflector at the bottom of the focusing lens. As the focusing lens moves away from the electronic deflector, the deformation at the bottom of the lens decreases from the order of nm at 10 mm to the order of 10-4 nm at 60 mm. This indicates that to avoid the influence of the magnetic field of the electronic deflector on the optical performance of the focusing lens, the electronic deflector should be at least 10 mm away from the bottom of the focusing lens.

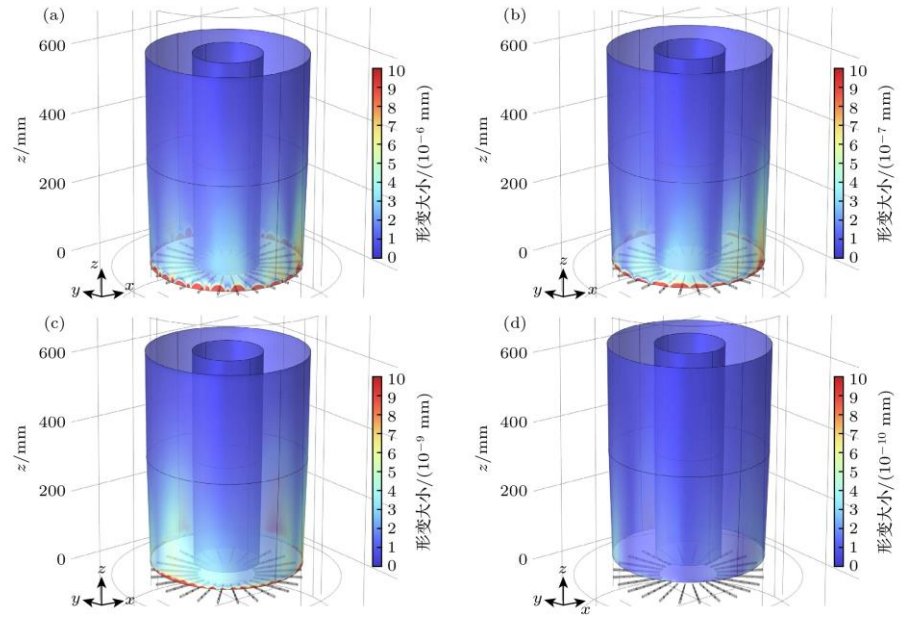

Figure 18. Deformation of the focusing telescope mirrors when the distance between the mirror bottom and electron deflector is (a) 10 mm, (b) 20 mm, (c) 40 mm, and (d) 60 mm.

The above simulation results show that the design parameters of the NdFeB magnet structure of the electron deflector fully meet the deflection requirements of the eXTP focusing mirror optical system for low-energy electrons, and the electron deflection efficiency of 100% can be achieved for 25 keV electrons within the incident angle of ± 5 ° and the deflection distance of 5250 mm.

3. Conclusion

In this paper, the finite element analysis software COMSOL Multiphysics is used to establish the physical simulation model of the electronic deflector and the focusing lens for the development of the eXTP focusing lens electronic deflector. The magnetic induction distribution, the electronic deflection trajectory and the influence of the magnetic field on the focusing lens are analyzed, and the electromagnetic parameters of the electronic deflector are designed. The simulation results show that the magnetic induction in the space around the electron deflector decreases along the radius direction, and the maximum magnetic induction in the middle of the two spokes can reach 0.027 T. In the plane and longitudinal distribution of magnetic flux density, when the radius is greater than 280 mm or the longitudinal distance is greater than 60 mm, the magnetic flux density is less than 5×10^{-5} T (0. 5 Gs), which meets the design requirements of electromagnetic compatibility. When the incident angle is less than 10 °, the electron deflection efficiency decreases with the increase of electron energy and incident angle, and the electron deflection efficiency can reach 100% below 50 keV, which meets the design requirements of electron deflection. When the bottom of the focusing lens is 130 mm away from the electronic deflector, the stress of the focusing lens under the action of the magnetic field is only 10^{-3} N/m^2, and the deformation is only 10^{-5} nm, which indicates that the magnetic field does not affect the optical performance of the focusing mirror. The above simulation analysis shows that the design parameters of the NdFeB magnet structure of the electron deflector fully meet the deflection requirements of the eXTP focusing mirror optical system for low-energy electrons, and the electron deflection efficiency of 100% can be achieved for 25 keV electrons with an incident angle within ± 5 ° and a deflection distance of 5250 mm, which provides an important reference for the development of the eXTP focusing mirror electron deflector. In addition, the mechanical reliability of the overall structure of the electronic deflector has not been considered in the existing research. In the future, the modal analysis and vibration response analysis of the electronic deflector under satellite mechanical conditions will be carried out to further optimize the mechanical structure of the hub of the electronic defector.

References

[1] Yuan W M, Zhang C, Chen Y, Sun S L, Zhang Y H, Cui W, Lin Z X, Huang M H, Zhao D H, Wang W X, Qiu Y L, Liu Z, Pan H W, Cai H B, Deng J S, Jia Z Q, Jin C C, Sun H, Hu H B, Liu F F, Zhang M, Song L M, Lu F J, Jia S M, Li C K, Zhao H S, Ge M Y, Zhang J, Cui W W, Wang Y S, Wang J, Sun X J, Jin G, Li L H, Chen F S, Cai Z M, Guo T, Liu G H, Liu H Q, Feng H, Zhang S N, Zhang B, Dai Z G, Wu X F, Gou L J 2018 *Sci. China: Phys. Mech.* **48** 039502

[2] Jeong S, Panasyuk M I, Reglero V 2018 *Space Sci. Rev.* **214** 25

[3] Zhang S N, Santangelo A, Feroci M 2019 *Sci. China Phys. Mech.* **62** 25

[4] Zand J J M, Bozzo E, Qu J L 2019 *Sci. China Phys. Mech.* **62** 029506

[5] Aslanyan V, Keresztes K, Feldman C, Pearson J F, Willingale R, Martindale A, Sembay S, Osborne J P, Sachdev S S, Bicknell C L, Houghton P R, Crawford T, Chornay D 2019 *Rev. Scientif. Inst.* **90** 124502

[6] Zhang S N, Santangelo A, Feroci M, et al. 2018 *Sci. China: Phys. Mech.* **62** 029502

[7] Yuan W M, Zhang C, Feng H, et al. 2015 *Swift: 10 Years of Discovery*

[8] Yuan W M, Chen Z, Ling Z, et al. 2018 *Proc. SPIE: Space Telescopes and Instrumentation 2018: Ultraviolet to Gamma Ray* **2018** 1069925

[9] Chen Y, Cui W W, Han D W, et al. 2020 *Proc. SPIE: Space Telescopes and Instrumentation 2020: Ultraviolet to Gamma Ray* **2020** 11444B

[10] Gehrels N, Chincarini G, Giommi P, et al. 2004 *Astrophys. J.* **611** 1309

[11] Willingale R 2000 *An electron diverter for the Swift Telescope XRA study note XRT-LUX-RE-011/1* （University of Leicester

[12] Friedrich P, Br äuninger H, Budau B, et al. 2012 *Proc. SPIE* **8443** 84431S

[13] Spiga D, Fioretti V, Bulgarelli A, et al. 2008 *Proc. SPIE: Space Telescopes and Instrumentation 2008: Ultraviolet to Gamma Ray* 7011 70112Y

[14] Wang L, Qin L, Cheng J, et al. 2020 *IEEE Trans. Appl. Supercond.* **30** 1

[15] Lotti S, Mineo T, Jacquey C, et al. 2018 *Exp. Astron.* **45** 411

[16] Fioretti V, Bulgarelli A, Molendi S, et al. 2018 *Astrophys. J.* **867** 9

[17] Qi L Q, Li G, Xu Y P, et al. 2020 *Nucl. Instrum. Meth. A* **963** 163702

[18] Qi L Q, Li G, Xu Y P, Chen Y, He H L, Wang Y S, Yang Y J, Zhang J, Lu F J 2021 *Exp. Astron.* **51** 475

[19] Aguilar M, Alcaraz J, Allaby J, et al. 2002 *Phys. Rep.* **366** 331

[20] Aguilar M, Cavasonza L A, Ambrosi G, et al. 2021 *Phys. Rep.* **894** 1